molecular pharmaceutics

Article

Cite This: Mol. Pharmaceutics 2019, 16, 724−736

pubs.acs.org/molecularpharmaceutics

Targeted Mitochondrial COQ_{10} Delivery Attenuates Antiretroviral-Drug-Induced Senescence of Neural Progenitor Cells

Martina Velichkovska,[†] Bapurao Surnar,[†] Madhavan Nair,[‡] Shanta Dhar,[†,§] and Michal Toborek*[,†]

[†]Department of Biochemistry and Molecular Biology and [§]Sylvester Comprehensive Cancer Center, University of Miami Miller School of Medicine, Miami, Florida, United States

[‡]Department of Immunology, Herbert Wertheim College of Medicine, Florida International University, Miami, Florida, United States

ABSTRACT: HIV infection is associated with symptoms of accelerated or accentuated aging that are likely to be driven not only by HIV itself but also by the toxicity of long-term use of antiretroviral drugs. Therefore, it is crucially important to understand the mechanisms by which antiretroviral drugs may contribute to aging. The aim of this study was to investigate the hypothesis that antiretroviral drugs cause increased reactive oxygen species (ROS) generation that results in mitochondrial dysfunction and culminates in promoting cellular senescence. In addition, we applied targeted nanoparticle (NP)-based delivery to specifically enrich mitochondria with coenzyme Q_{10} (CoQ_{10}) in order to enhance antioxidant protection. The studies employed neural progenitor cells (NPCs), as differentiation of these cells into mature neurons is affected both during HIV infection and in the aging process. Exposure of cultured NPCs to various combinations of HIV antiretroviral therapy (ART) induced a more than 2-fold increase in mitochondrial ROS generation and mitochondrial membrane potential, a more than 50% decrease in oxygen consumption and ATP levels, a 60% decrease in SIRT3 expression, and a 42% decrease in cell proliferation relative to control levels. These alterations were accompanied by a 37% increase in beta-galactosidase staining and a shortening of the telomere length to more than half of the length of controls as assessed by quantitative telomere-FISH labeling, indicating accelerated NPC senescence in response to ART exposure. Importantly, CoQ_{10} delivered by targeted nanoparticles effectively attenuated these effects. Overall, these results indicate that ART promotes cellular senescence by causing mitochondrial dysfunction, which can be successfully reversed by supplementation with mitochondria-targeted CoQ_{10}.

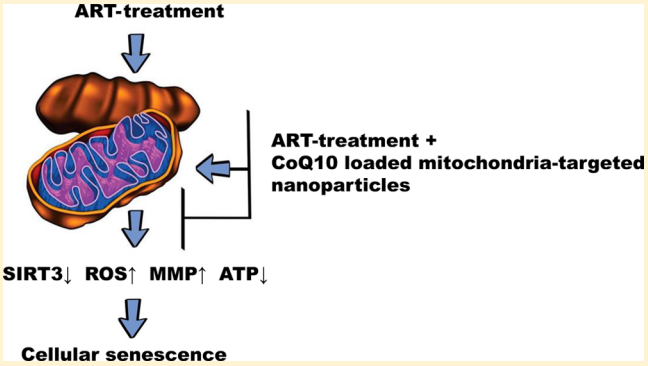

KEYWORDS: *aging, antiretroviral therapy, CoQ_{10}, HIV, mitochondria, oxidative stress, progenitor cells*

INTRODUCTION

Even though HIV patients nowadays have nearly normal life expectancy due to the advent of antiretroviral drugs, HIV-associated neurocognitive disorders (HANDs) and other comorbidities remain an unresolved health problem.[1] Up to 70% of HIV positive individuals develop neurological complications of the central nervous system[2] and experience accelerated aging 15−20 years earlier than noninfected controls.[3] While these comorbidities might be induced by long-term replication of HIV in the CNS,[4] HIV antiretroviral therapy (ART) has also been reported as a possible contributing factor to the neurocognitive complications.[5] The ability of ART to successfully control viral load has unquestionable positive effects; nevertheless, supplementation of antiretroviral drugs with neuroprotective agents has been proposed in order to decrease their toxicity.[6−8] For this purpose, it is of crucial importance to identify the right targets through which ART may accelerate the process of aging, thus contributing to the development of HANDs.

Mitochondrial dysfunction, leading to oxidative stress, is a reoccurring feature of many diseases associated with aging[8−10] and is also involved in ART-induced toxicity.[11−13] Hence, we hypothesized that antiretroviral drugs can compromise the functionality of neural progenitor cells (NPCs) and contribute to cellular senescence by causing damage to mitochondria.

Taking into consideration the role of oxidative stress in aging, we introduced supplementation of ART with antioxidant CoQ_{10} that is also a member of the electron transport chain. Indeed, compromised mitochondrial function has been shown to be successfully reversed after supplementation with CoQ_{10}.[14] CoQ_{10} was also shown to exert its protective effects on the process of aging through pathways that include SIRT3 activation.[15]

Received: September 28, 2018
Revised: December 10, 2018
Accepted: December 28, 2018
Published: December 28, 2018

DOI: 10.1021/acs.molpharmaceut.8b01014
Mol. Pharmaceutics 2019, 16, 724−736

While CoQ_{10} is able to freely diffuse across cellular membranes, it is notoriously difficult to ensure its efficient mitochondrial delivery. Therefore, most studies have reported the usage of very high levels of CoQ_{10} in order to achieve therapeutic concentrations. It was suggested[14] that doses of more than 10 μM CoQ_{10} are needed to restore the activity of electron transport chain enzymes. Because such high levels would be challenging, if not impossible, to achieve by standard supplementation, we employed a mitochondria-targeted nanoparticle (NP)-based strategy for CoQ_{10} delivery. The obtained results indicate that such a strategy can reduce ART-induced mitochondrial dysfunction and attenuate the impact of antiretroviral drugs on accelerated senescence of NPCs.

EXPERIMENTAL PROCEDURES

Cell Culture. Mouse neural progenitor cells (NPCs; NE4C cell line, ATCC, USA) were cultured following the manufacturer's protocols on dishes coated with poly-L-lysine solution (Sigma, USA) at 5% CO_2 and 37 °C, in MEM medium (Sigma, USA) supplemented with glutamine (Gibco Life Technologies, USA) and 0.5% FBS (Thermo Fisher Scientific, USA). Human neural progenitor cells (ReNcell VM cell line, Millipore, USA) were grown on laminin-coated dishes in maintenance media (Millipore, USA), supplemented with 20 ng/mL EGF and 20 ng/mL FGF-2 (Millipore, USA), following the manufacturer's protocols. For live confocal imaging with water immersion lenses (Olympus Fluoview 2000), cells were grown on 35 mm dishes; for the Seahorse assay (Agilent, USA), cells were cultured on Seahorse XF96 Cell Culture microplates, for spectrofluorometric ROS and the mitochondrial membrane potential quantification, cells were grown on bottom opaque plates (Greiner BioOne, USA), for beta-galactosidase assay cells were grown on 6-well plates, and for SIRT3 expression, BrdU incorporation, and telomere-FISH assays, cells were cultured either on 6-well plates containing removable glass slides on the bottom or on 8-well chamber slides.

HIV Infections. Infection of mouse NPCs was performed with Eco-HIV (a gift from Dr. David Volsky, Icahn School of Medicine at Mount Sinai, New York, NY), a mutant strain of HIV adapted for mouse cells. The HIV gp120 envelope protein in this strain was replaced with the murine leukemia virus gp80 envelope protein. Eco-HIV stock was obtained by transfecting HEK 293T cells with Eco-HIV plasmids overnight and allowing the cells to grow for the following 3 days in DMEM media. Then, the supernatants were collected and passed through a 0.22 m filter. HIV titers were estimated on the basis of p24 HIV antigen measurements by ELISA (Zeptometrix). NPCs are susceptible to HIV infection, as demonstrated in our earlier study.[16] Infection was achieved by incubation of cells with Eco-HIV at 60 ng of p24/mL for 24 h.[16,17] Then, the virus was washed out and infection was verified by measuring p24 antigen levels.

Antiretroviral Drugs. The antiretroviral drugs used (ApexBio, USA) were combined and used as one of the following mixtures: Tenofovir and Emtricitabine (T+E; both nucleoside reverse transcriptase inhibitors, NRTIs), Tenofovir, Emtricitabine, and Raltegravir (T+E+Ral; NRTIs plus protease inhibitor), or Tenofovir, Emtricitabine, Ritonavir, and Darunavir (T+E+R+D; NRTIs plus integrase inhibitors). Tenofovir was used at 1 μM, Raltegravir at 2 μM, Davunavir at 12.9 μM, Emtricitabine at 5 μM, and Ritonavir at 0.7 μM, as final concentrations in the cell culture media. These concentrations are in the range of the typical plasma levels of these drugs in patients on ART. For the drugs that had to be diluted in DMSO, the final DMSO concentration was lower than 0.1%. Initial experiments included a control group that contained 0.1% DMSO in the medium, confirming that the effects observed are not due to DMSO. All drug combinations represent mixtures that are currently in clinical use.

CoQ_{10} Loaded Nanoparticles (CoQ_{10}-NPs). A dual function, brain accumulating and mitochondrion-targeted nanoparticle (NP) was developed by encapsulating mitochondria-acting antioxidant CoQ_{10} using a biocompatible polymer poly(lactic-*co*-glycolic acid) (PLGA)-block (*b*)-polyethylene glycol (PEG) functionalized with a terminal lipophilic triphenylphosphonium (TPP) cation.[18,19,22] This targeted NP is abbreviated as T-CoQ_{10}. The nontargeted NPs were prepared using PLGA-*b*-PEG-OH and are abbreviated as NT-CoQ_{10}. All NPs were prepared by a nanoprecipitation method using protocols previously developed by us.[18−22] PLGA-*b*-PEG-TPP polymer-based NPs were employed, because TPP contributes to directing these particles to the mitochondria by taking advantage of the substantial negative mitochondrial membrane potential ($\Delta\psi$m) that exists across the inner mitochondrial membrane (IMM).[18,19,22] The brain accumulating properties of these particles and their ability to penetrate the blood−brain barrier (BBB) were demonstrated in earlier publications.[18,20,22] Stock solutions of the polymer were made by dissolving 5 mg of the polymer and 1 mg of CoQ_{10} in 1 mL of dimethylformamide (DMF). This solution was added dropwise to 10 mL of nanopure water stirring at 900 rpm. This solution was stirred for 2 h at room temperature. These NPs were purified by centrifugation using 100 kDa amicon centrifugation devices and washing three times with water at 2800 rpm, 4 °C. The purified NPs were resuspended in nanopure water and characterized using dynamic light scattering (DLS) for diameter, surface charge, and polydispersity index. The amount of CoQ_{10} in the NPs was quantified by HPLC applying a wavelength of 284 nm using a mixture of methanol (40%) and isopropanol (60%) as a mobile phase. The T-CoQ_{10} and NT-CoQ_{10} were found to be 140 ± 1.7 and 122 ± 1.5 nm in diameter, respectively. The T-CoQ_{10}'s were positively charged with a zeta potential of 50 ± 0.9 mV, and the NT-CoQ_{10}'s were negatively charged with a zeta potential of −20 ± 0.4 mV. The polydispersity indexes (PDIs) for T-CoQ_{10} and NT-CoQ_{10} were found as 0.223 ± 0.0001 and 0.230 ± 0.005, respectively. The percent loading of CoQ_{10} was found to be 9.0 and 10 for T-CoQ_{10} and NT-CoQ_{10}, respectively. These percent loadings correspond to an encapsulation efficiency of 45 and 51% for T-CoQ_{10} and NT-CoQ_{10}, respectively.

% Loading and % EE of CoQ_{10} was calculated using the following formulas:

$$\%\ \text{Loading of } CoQ_{10} = (\text{Weight of } CoQ_{10} \text{ in NPs})/\text{Total weight of NPs} \times 100$$

$$\%\text{EE of } CoQ_{10} = (\text{Weight of } CoQ_{10} \text{ in NPs})/\text{Feed weight of } CoQ_{10} \times 100$$

CoQ_{10} Treatment. Cells were pretreated with free CoQ_{10} (Sigma, USA), nontargeted nanoparticles loaded with CoQ_{10} (NT-CoQ_{10}-NPs), or mitochondria-targeted nanoparticles loaded with CoQ_{10} (T-CoQ_{10}-NPs) for 24 h, followed by

DOI: 10.1021/acs.molpharmaceut.8b01014
Mol. Pharmaceutics 2019, 16, 724−736

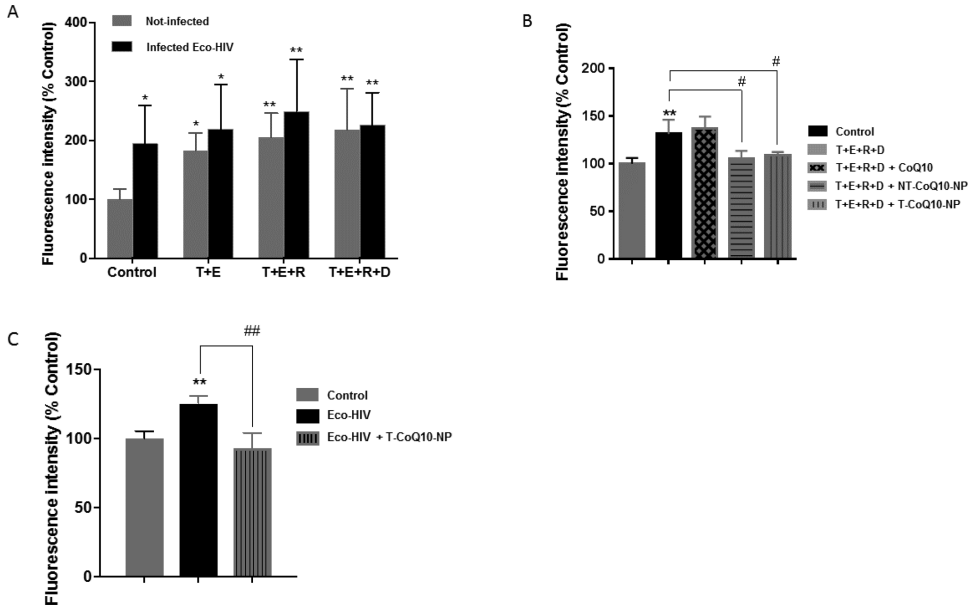

Figure 1. ART-induced generation of reactive oxygen species (ROS) is reversed by CoQ_{10}-NP formulations. (A) Noninfected and Eco-HIV-infected mouse NPCs were treated with the indicated combinations of antiretroviral drugs for 3 h, and generation of ROS was assessed by spectrofluorometric quantification of DCF fluorescence. (B) Cells were pretreated with 500 nM CoQ_{10} for 24 h as a free drug or loaded into nanoparticles (NPs) that were either mitochondria-targeted (T-CoQ_{10}-NPs) or nontargeted (NT-CoQ_{10}-NPs), followed by exposure to the mixture of Tenofovir, Emtricitabine, Ritonavir, and Darunavir, a representative antiretroviral combination of ART. (C) Cells were pretreated with 500 nM CoQ_{10} loaded into mitochondria-targeted nanoparticles (T-CoQ_{10}-NPs), followed by Eco-HIV infection for 24 h. All results are mean + SEM, n = 9−10 per group. Abbreviations: D, Darunavir; E, Emtricitabine; R, Ritonavir; T, Tenofovir. *Indicates significant differences between the control and the respective treatment groups at $p < 0.05$; **, $p < 0.01$. #Indicates significant differences between the ART and the ART+CoQ_{10} groups at $p < 0.05$; ##, $p < 0.01$.

antiretroviral treatment for different time points as specified in the respective experiments. The same dose of CoQ_{10} of 500 nM, which was determined to be optimal with preliminary experiments, was used in all experiments to compare the efficiency of mitochondrial delivery. The stock solution of synthesized NPs was in micromolar concentrations that were diluted to the working concentration of 500 nM CoQ_{10} by adding it to cell culture media.

Mitochondrial Membrane Potential, Spectrofluorometric Quantifications of ROS, and MitoSOX Staining. Tetramethylrhodamine ethyl ester (TMRE; Thermo Fisher Scientific, USA), the fluorescent dye sequestering in active mitochondria, was added along with nuclear marker dyes Hoechst (Thermo Fisher Scientific, USA) and Mitotracker Green (Thermo Fisher, USA) in order to quantify the mitochondrial membrane potential.

To quantify the generation of ROS, H2-DCFDA (Thermo Fisher Scientific, USA), which converts into DCFDA and measures hydroxyl, peroxyl, and other ROS (with the exception of superoxide radicals), was added to the culture media with the nucleic acid stain DRAQ-5 (Thermo Fisher Scientific, USA). After 30 min of incubation, followed by two extensive washes, fluorescence was measured by a Gemini EM spectrofluorometer (Molecular Devices, USA). The area under the curve for the recorded spectral range was used for quantification, and the results were normalized to Hoechst or DRAQ-5 fluorescence intensity. Titration experiments were performed for DCF and TMRE, and the lowest concentrations that produced a signal were used for both dyes. Additionally, when performing the experiments, media containing antiretroviral drugs were exchanged into fresh medium.

For MitoSOX staining, the cells were grown on 35 mm plates and stained with MitoSOX Red (Thermo Fisher, USA) for 10 min at 37 °C and Hoechst to visualize the nuclei. After incubation, the cells were washed and live images were acquired with water-immersed lenses by a confocal microscope (Olympus, Fluoview).

Seahorse Assay. The Seahorse Mito Stress measurements were performed as instructed by the manufacturer (Agilent, USA). Cells were grown on Seahorse XF96 Cell Culture microplates and treated with CoQ_{10} and/or ART. Seahorse medium supplemented with 1 mM pyruvate, 2 mM glutamine, and 10 mM glucose was added to the plates 1 h before reading, and the assay was performed in three repeats 3 min−0.5 min−3 min mix−wait−measure cycles after injecting 1 μM oligomycin, 1 μM carbonyl cyanide 4-(trifluoromethoxy) phenylhydrazone (FCCP), and 0.5 μM rotenone and antimycin. The Seahorse XF96 Analyzer was used for measurements, and the results were analyzed by the Wave software and Mito Stress Report Generator (Agilent, USA).

BrdU Immunostaining, Senescence-Associated Beta-Galactosidase Assay, and Telomere FISH Quantification. For bromodeoxyuridine (BrdU) immunostaining that assesses cell proliferation, plates were incubated with BrdU labeling solution (Thermo Fisher Scientific, USA) for 3 h, fixed with 4% paraformaldehyde (PFA), and permeabilized with 0.1% Triton-X. Then, DNA was hydrolyzed by incubating with 2 M HCl for 30 min, followed by neutralizing with 0.1 M sodium borate. Subsequently, blocking and immunostaining were performed using anti-BrdU primary antibody (1:200, Roche Applied Science) for overnight incubation and red-conjugated Alexa-Fluor 594 (1:400, Thermo Fisher, USA) as a secondary antibody for 1 h incubation. Nuclei were stained with Hoechst (1:2000), and the slides were imaged with a confocal microscope.

Cellular senescence was assayed by a beta-galactosidase staining kit (Cell Signaling, USA) as described by the

DOI: 10.1021/acs.molpharmaceut.8b01014
Mol. Pharmaceutics 2019, 16, 724−736

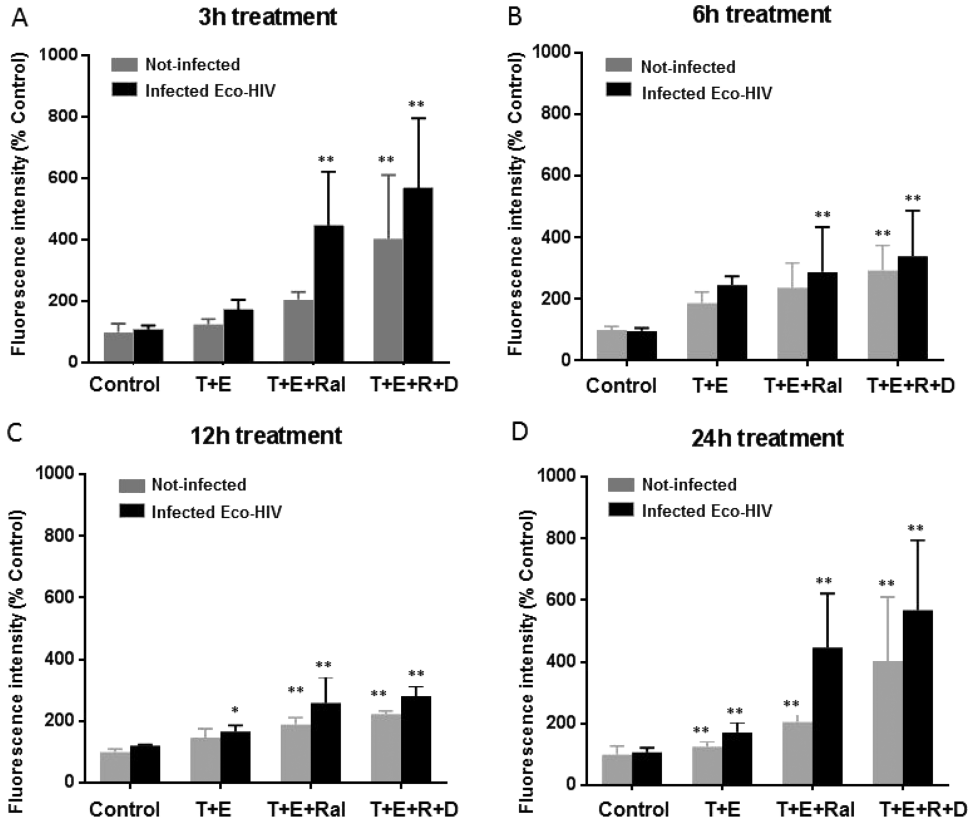

Figure 2. ART treatment alters mitochondrial membrane potential (MMP). Noninfected and Eco-HIV-infected mouse NPCs were treated with the indicated combinations of antiretroviral drugs for 3 h (A), 6 h (B), 12 h (C), or 24 h (D). MMP was evaluated by spectrofluorometric quantification of TMRE fluorescence, normalized to Mitotracker fluorescence and Hoechst fluorescence. All results are mean + SEM, $n = 5$ per group. Abbreviations as in Figure 1; Ral, Raltegravir. *Indicates significant differences between the control and the respective treatment groups at $p < 0.05$; **, $p < 0.01$.

manufacturer. Briefly, cells were fixed and then stained with beta-galactosidase solution at pH 6. Following an overnight incubation, the cultures were washed, and images were acquired with light microscopy.

Telomere length, measured by telomere FISH quantification, is another approach to assess cellular senescence. Cultures grown on slides were incubated with colcemid for 2.5 h, followed by cell harvesting, incubation with 75 mM KCl, and then an overnight incubation with 3:1 (v:v) methanol:acetic acid (Sigma, USA). The next day, cultures were treated with 4% PFA, followed by incubation with RNase and 0.005% pepsin (Sigma, USA). After dehydration with ethanol, slides were prewarmed and hybridized in a buffer containing a TelC (CCCTAA) probe (PnaBio, USA). After washing, nuclei were stained with Hoechst, and slides were imaged acquiring z-stacks by confocal microscopy. Quantification based on fluorescence intensity was performed using ImageJ (NIH, USA).

SIRT3 Immunostaining. Cells were grown on eight-well chamber slides, fixed with 4% PFA, permeabilized with 1% Triton X-100 for 30 min, and blocked with 20% Normal Goat Serum for 30 min. Subsequently, they were incubated overnight with anti-SIRT3 antibody (1:100, Cell Signaling, USA) at 4 °C. The next day, the primary antibody was labeled with red-conjugated secondary antibody Alexa-Fluor 594 (1:400, Thermo Fisher, USA) by incubation for 1 h. Mitotracker Green (Thermo Fisher, USA) was used for labeling the mitochondria, and Hoechst was used to visualize the nuclei. Both dyes were mixed and added to slides for 15 min of incubation. Images were acquired by a confocal microscope with z-stacks (Olympus, Fluoview 2000).

Statistical Analysis. All data sets were organized in Excel (Microsoft) and exported to Prism v.6 (GraphPad software) to determine statistical significance. One-way or two-way ANOVA was used, depending on the specific experiment. * indicates significant difference ($p < 0.05$) as compared with the treatment groups to nontreated/noninfected controls, while # indicates significant difference ($p < 0.05$) between the ART and ART +CoQ_{10} treated groups.

RESULTS

ART-Induced Generation of ROS Is Reversed by CoQ_{10}-NP Formulations. Figure 1 indicates the impact of various therapeutically relevant ART mixtures (Tenofovir, T; Emtricitabine, E; Ritonavir, R; Darunavir, D) on ROS generation in noninfected and Eco-HIV-infected mouse NPCs as measured by DCF fluorescence. The results were normalized to the intensity of nuclear staining with DRAQ-5. Cells were treated with antiretroviral drug combinations for 1.5−3 h at the concentrations specified in the Experimental Procedures section. Both Eco-HIV infection and the exposure to all ART combinations resulted in an increase in ROS generation as compared to noninfected, vehicle treated controls (Figure 1A). Relatively, the highest increase in ROS levels was observed in cells treated with the combination of T+E+R+D. No differences were observed between the impact of ART in noninfected and infected cultures due to relatively high standard deviation data.

The T+E+R+D ART combination was next employed to evaluate the impact of CoQ_{10} formulations (Figure 1B). Cells were pretreated for 24 h with CoQ_{10} at 500 nM either in a free

DOI: 10.1021/acs.molpharmaceut.8b01014
Mol. Pharmaceutics 2019, 16, 724−736

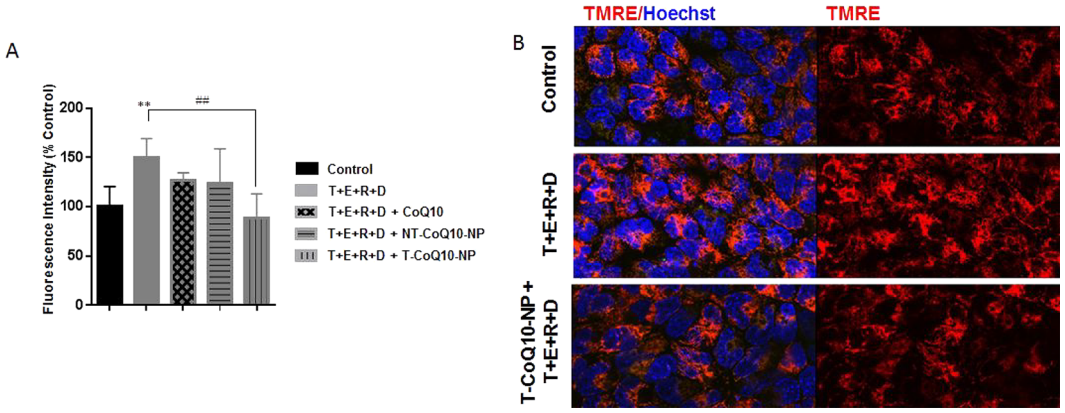

Figure 3. Mitochondria-targeted CoQ_{10}-NP formulations attenuate ART-induced alterations of mitochondrial membrane potential. (A) Mouse NPCs were pretreated with 500 nM CoQ_{10} for 24 h as a free drug or loaded into nanoparticles (NPs) that were either mitochondria-targeted (T-CoQ_{10}-NPs) or nontargeted (NT-CoQ_{10}-NPs), followed by exposure to the mixture of Tenofovir, Emtricitabine, Ritonavir, and Darunavir (T+E+R+D), a representative antiretroviral combination of ART. MMP was evaluated as in Figure 2. All results are mean + SEM, n = 9−10 per group. **Indicates significant differences between the control and the ART group at $p < 0.01$. ##Indicates significant differences between the ART and the ART+CoQ_{10} groups at $p < 0.01$. (B) Representative images from confocal live microscopy for visualizing TMRE (red) staining and Hoechst (blue) fluorescence. Cells were pretreated with mitochondria-targeted CoQ_{10}-NPs (T-CoQ_{10}-NPs) for 24 h, followed by Tenofovir, Emtricitabine, Ritonavir, and Darunavir (T+E+R+D) exposure for another 24 h. Abbreviations as in Figure 1.

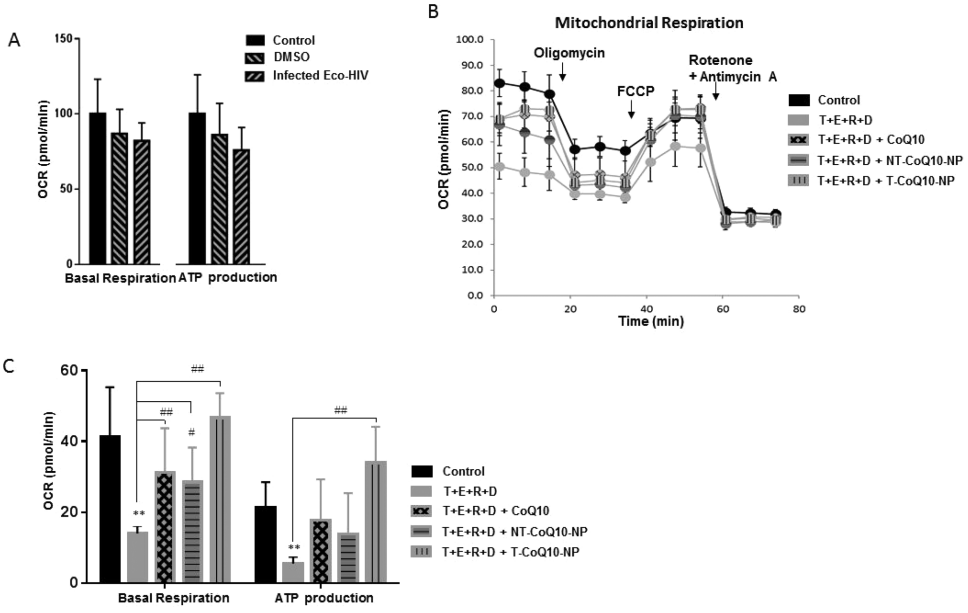

Figure 4. CoQ_{10}-NP formulations protect against ART-induced mitochondrial dysfunction. (A) Mouse NPCs were infected with Eco-HIV or exposed to medium containing 0.1% DMSO, which was used for dissolving ART in panels B and C, and basal respiration and ATP levels were assessed by the Seahorse method. (B and C) Mouse NPCs were pretreated with 500 nM CoQ_{10} for 24 h as a free drug or loaded into nanoparticles (CoQ_{10}-NPs) that were either mitochondria-targeted (T-CoQ_{10}-NPs) or nontargeted (NT-CoQ_{10}-NPs), followed by exposure to the mixture of Tenofovir, Emtricitabine, Ritonavir, and Darunavir (T+E+R+D). The mitochondrial respiration profile (B) that was used to calculate basal respiration and ATP levels (C) was assessed by the Seahorse method. All results are mean + SEM, n = 7−9 per group. *Indicates significant differences between the control and the ART group at $p < 0.05$; **, $p < 0.01$. #Indicates significant differences between the ART and ART+CoQ_{10} groups at $p < 0.05$; ##, $p < 0.01$. Abbreviations as in Figure 1.

form or loaded into mitochondria-targeted or nontargeted NPs (T-CoQ_{10}-NPs or NT-CoQ_{10}-NPs, respectively). The addition of free CoQ_{10} had no significant effect on ART-induced ROS levels. In contrast, both T-CoQ_{10}-NPs and NT-CoQ_{10}-NPs significantly attenuated ART-induced ROS generation. No differences in antioxidative protection were observed between T-CoQ_{10}-NPs and NT-CoQ_{10}-NPs. T-CoQ_{10}-NPs were also protective against Eco-HIV-induced ROS generation in NPCs. As illustrated in Figure 1C, pretreatment of NPCs with 500 nM CoQ_{10} loaded into T-CoQ_{10}-NPs effectively protected against cellular oxidative stress.

ART Treatment Alters Mitochondrial Membrane Potential (MMP). Mitochondrial dysfunction may underlie the toxicity of antiretroviral drugs. Therefore, we next evaluated the impact of therapeutically relevant ART combinations (abbreviations as in Figure 1, plus Raltegravir) on MMP in noninfected and HIV-infected NPC cultures (Figure 2). Exposure to antiretroviral drugs resulted in a marked increase in MMP, indicating membrane hyperpolarization, with the T+E

DOI: 10.1021/acs.molpharmaceut.8b01014
Mol. Pharmaceutics 2019, 16, 724−736

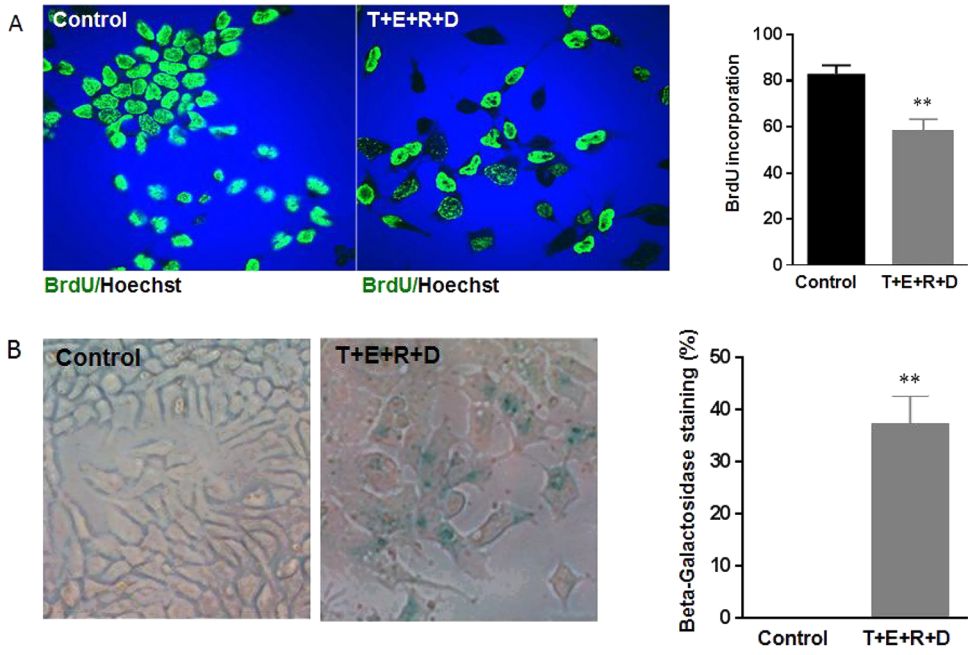

Figure 5. ART decreases proliferation and induces senescence of NPCs. Mouse NPCs were exposed to the mixture of Tenofovir, Emtricitabine, Ritonavir, and Darunavir (T+E+R+D) for 24 h. (A) Cell proliferation was assessed by BrdU fluorescence and counterstaining with Hoechst; left panel, representative immunofluorescence images; right panel, quantitative results obtained by counting the number of nuclei with positive BrdU staining. (B) Cellular senescence was assessed by the β-galactosidase assay; left panel, representative images of the staining; right panel, quantitative results. All results are mean + SEM, $n = 5-10$ per group. **Indicates significant differences between the control and the ART group at $p < 0.01$. Abbreviations as in Figure 1.

+R+D combination having the most significant effect. The toxic effect of this ART combination was observed at early (3 h) and prolonged (24 h) exposure times. The T+E+R combination was also toxic, however, to a lesser degree than the T+E+R+D mixture. In contrast, the T+E combination appeared to be safer and only slightly, although significantly, affected MMP after a 24 h exposure.

While infection with Eco-HIV alone did not influence MMP as compared to noninfected and vehicle-treated controls, ART-induced mitochondrial hyperpolarization was much more pronounced in infected than in noninfected cultures. For example, the T+E+R mixture at 3 or 6 h of treatment affected MMP only in infected but not in noninfected cells (Figure 2A and B). Even though the difference in infected cultures as compared to noninfected controls in all studied time points was not statistically significant, there appeared to be an overall trend toward more pronounced MMP alternations after infection (Figure 2).

T-CoQ$_{10}$-NPs Attenuate ART-Induced Alterations of Mitochondrial Membrane Potential. In the next series of experiments, we evaluated the impact of CoQ$_{10}$ formulations on ART-induced hyperpolarization of the mitochondrial membrane as measured by mitochondrial dye, TMRE. Quantitative results were acquired using a fluorescence plate reader (Figure 3A). The T+E+R+D mixture was employed in these analyses as the ART combination that resulted in the most pronounced alterations of MMP. When added in a free form, CoQ$_{10}$ resulted only in a nonsignificant trend toward attenuation of changes in TMRE expression. Similarly, NT-CoQ$_{10}$-NP delivery was ineffective against ART-induced alterations of MMP. Only the T-CoQ$_{10}$-NP delivery restored the mitochondrial membrane potential levels in ART-treated NPCs to the same level as in the control group (Figure 3A). The images illustrated in Figure 3B were acquired with confocal microscopy employing the same dyes that were used for quantitative analyses in order to provide a visual representation of mitochondrial hyperpolarization and the protective impact of targeted CoQ$_{10}$-NP delivery.

CoQ10-NP Formulations Protect against ART-Induced Mitochondrial Dysfunction. We then evaluated the impact of ART on mitochondrial function using the Seahorse assay. Infection with Eco-HIV did not alter basal respiration or ATP production in NPC cultures (Figure 4A); therefore, the impact of various CoQ$_{10}$ formulations was then assessed only in noninfected cultures exposed to the combination of T+E+R+D that was selected from previous experiments. The mitochondrial respiration profile for the noninfected groups (Figure 4B) showed an overall decrease in oxygen consumption rate after T+E+R+D exposure, and the trend was attenuated after pretreatment with various CoQ$_{10}$ formulations. The oxygen consumption rate results were then used to calculate mitochondrial basal respiration and ATP production levels using the Seahorse Software, Wave. Exposure to the T+E+R+D combination resulted in a decrease in mitochondrial basal respiration and ATP production levels (Figure 4C). Pretreatment with CoQ$_{10}$ in a free form was ineffective in preventing ART-induced changes in ATP production. In contrast, pretreatment with T-CoQ$_{10}$-NPs significantly restored ATP production (Figure 4C). While all three formulations of CoQ$_{10}$ successfully attenuated ART-induced changes in basal mitochondrial respiration, the most efficient protection was observed in cells pretreated with T-CoQ$_{10}$-NPs (Figure 4C).

ART Decreases Proliferation and Induces Senescence of NPCs. Mitochondrial dysfunction has been linked to aging; therefore, we evaluated the impact of ART and CoQ$_{10}$ formulations on proliferation and senescence of NPCs. Representative to ART, the T+E+R+D combination was used in this series of experiments. Figure 5A (left panel) illustrates BrdU incorporation into control and treated cells, and quantified

DOI: 10.1021/acs.molpharmaceut.8b01014
Mol. Pharmaceutics 2019, 16, 724−736

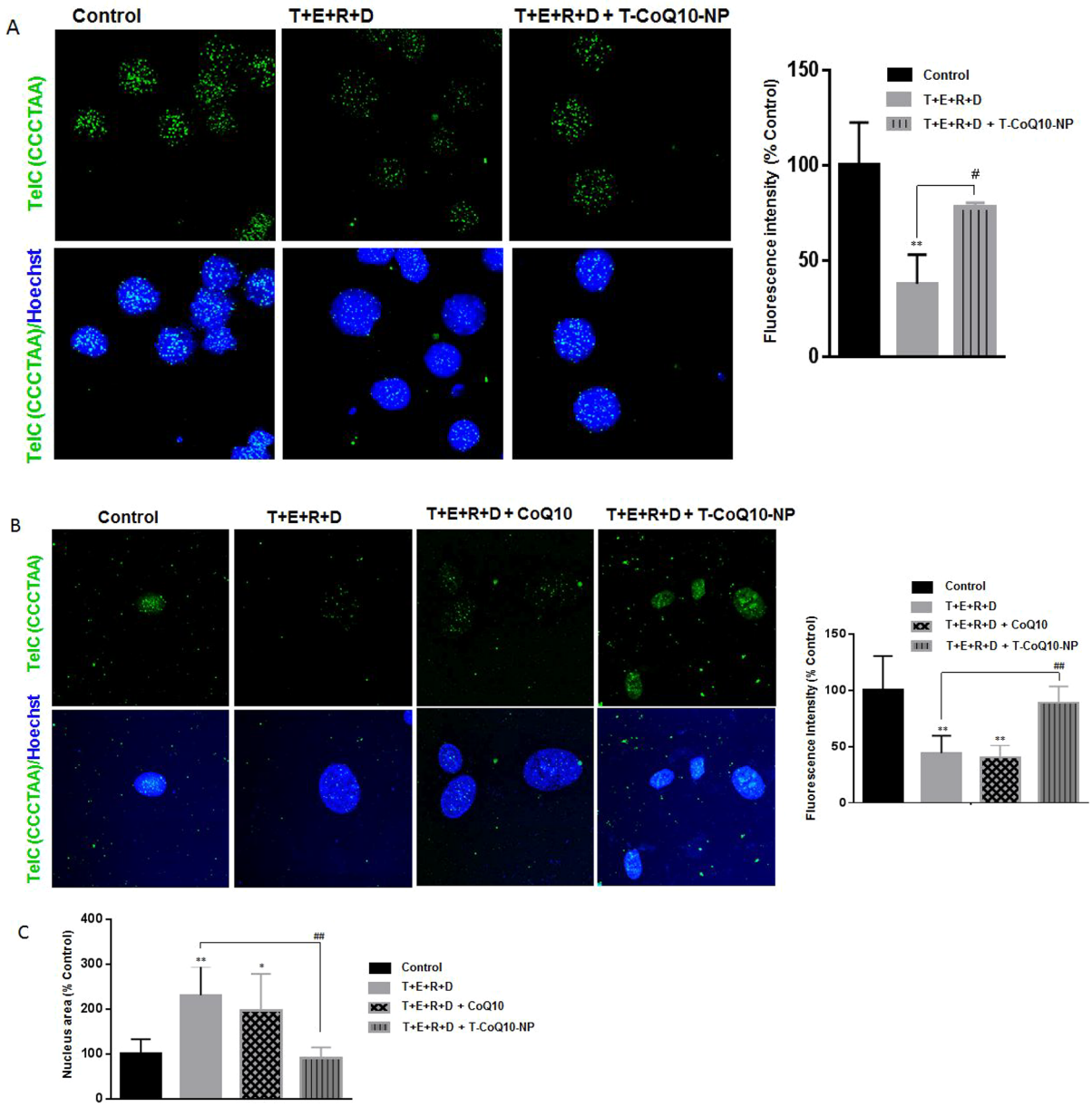

Figure 6. Mitochondria-targeted CoQ_{10}-NPs attenuate ART-induced shortening of telomeres. Mouse (A and B) and human (C−E) NPCs were pretreated with 500 nM CoQ_{10} for 24 h as a free drug or loaded into mitochondria-targeted nanoparticles (T-CoQ_{10}-NPs), followed by exposure to the mixture of Tenofovir, Emtricitabine, Ritonavir, and Darunavir (T+E+R+D). Telomere length was evaluated by quantitative FISH assay in mouse (A) or human (B) NPCs. The left panels in parts A and B visualize representative images for FISH assay, and the right panels represent quantitative results. (C) Quantified area of nuclei from part B. All results are mean + SEM, $n = 3-21$ per group. *Indicates significant differences between the control and the ART group at $p < 0.05$; **, $p < 0.01$. #Indicates significant differences between the ART and ART+CoQ_{10} groups at $p < 0.05$; ##, $p < 0.01$. Abbreviations as in Figure 1.

results of these experiments are presented in the right panel. Exposure to the T+E+R+D mixture for 48 h significantly decreased the NPC proliferation rate by 20%, as determined by BrdU incorporation assay. In addition, exposure to the same ART mixture for 72 h induced senescence of NPCs, as measured by a β-galactosidase assay. Representative images for positively stained senescence-associated β-galactosidase cells are shown in Figure 5B, left panel, and quantitative results from these experiments are presented in the right panel. As illustrated, approximately 40% of cultured NPCs entered the senescent stage as the result of exposure to the T+E+R+D ART combination.

T-CoQ_{10}-NPs Attenuate ART-Induced Shortening of NPC Telomeres. Telomere shortening occurs in response to cellular stress and is consistent with cellular senescence. Therefore, telomere length was also evaluated in the present study by quantitative FISH using a probe that has the ability to hybridize to the CCCTAA fragment of telomeres (Figure 6). Figure 6A, left panel, illustrates representative images of this assay, and the right panel presents quantitative results. Exposure of mouse NPCs to the T+R+E+D mixture for 72 h resulted in a significant shortening of telomere length by more than 50%. Importantly, pretreatment with T-CoQ_{10}-NPs effectively attenuated this effect, bringing telomere length close to control values.

DOI: 10.1021/acs.molpharmaceut.8b01014
Mol. Pharmaceutics 2019, 16, 724−736

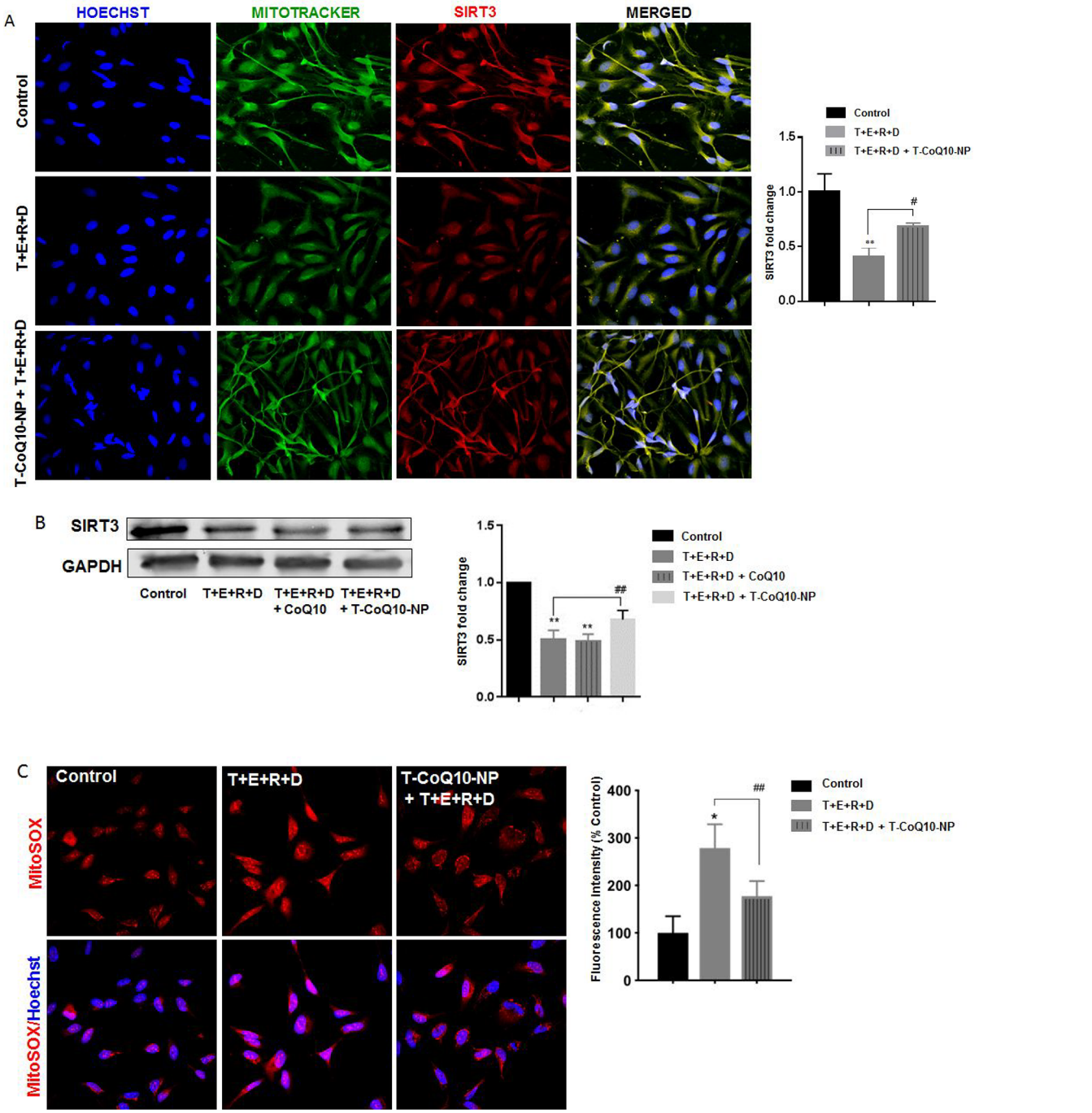

Figure 7. Mitochondria-targeted CoQ_{10}-NPs attenuate ART-induced alterations of SIRT3 expression. Human NPCs were pretreated with 500 nM CoQ_{10} for 24 h as mitochondria-targeted nanoparticles (T-CoQ_{10}-NPs), followed by exposure to the mixture of Tenofovir, Emtricitabine, Ritonavir, and Darunavir (T+E+R+D). SIRT3 expression was assessed by immunostaining. In addition, Hoechst and Mitotracker were used to stain the nuclei and mitochondria, respectively, in order to confirm mitochondrial localization of SIRT3. (A) Representative immunostaining images (left panel) and quantified results expressed as fold change relative to control (right panel). (B) Representative immunoblotting of SIRT3 (left panel); the blots were quantified by densitometry and statistical analyses, and the results were expressed as fold change relative to control (right panel). (C) Mitochondrial superoxide levels were assessed by live-cell staining with MitoSOX. The left panel visualizes representative images, and the right panel represents quantified results relative to the control. All results are mean + SEM, $n = 4$ per group. **Indicates significant differences between the control and the ART group at $p < 0.01$. ##Indicates significant differences between the ART and the ART+CoQ_{10} groups at $p < 0.01$. Abbreviations as in Figure 1.

These results were next fully reproduced in human NPCs (ReN cells) (Figure 6B). Exposure of these cells to the T+E+R+D mixture decreased telomere length by ~50%, the effect that was prevented by T-CoQ_{10}-NPs but not by CoQ_{10} used in a free form (Figure 6B, left panel, representative images, and right panel, quantitative results). Interestingly, exposure to this ART combination also increased the size of NPC nuclei (Figure 6C), further confirming the senescent phenotype. The impact of the T+E+R+D combination on the size of nuclei was also reversed by T-CoQ_{10}-NPs but not by a free form of CoQ_{10}.

T-CoQ_{10}-NPs Attenuate ART-Induced Alterations of SIRT3 Expression. One of the important enzymes responsible

DOI: 10.1021/acs.molpharmaceut.8b01014
Mol. Pharmaceutics 2019, 16, 724−736

for controlling proper mitochondrial functions is SIRT3; thus, expression of SIRT3 was also a subject of our studies. Immunostaining experiments with an anti-SIRT3 antibody showed that exposure to the T+E+R+D ART mixture for 48 h decreased expression of SIRT3 in human NPCs (Figure 7A; left panel, representative images, and right panel, quantitative results). Consistent with data from previous experiments on mitochondrial function, supplementation with T-CoQ_{10}-NPs attenuated these effects. We then confirmed these results in immunoblotting experiments. Cells were exposed to T+E+R+D in the presence or absence of CoQ_{10} or T-CoQ_{10}-NPs. As illustrated in Figure 7B (left panel, representative blot, and right panel, quantitative results), exposure to ART decreased SIRT3 protein expression. While pretreatment with the regular form of CoQ_{10} was ineffective, T-CoQ_{10}-NPs attenuated the impact of T+E+R+D on SIRT3 protein expression.

Because SIRT3 is involved in the protection against mitochondrial oxidative stress, we next evaluated mitochondrial superoxide levels by staining with MitoSOX (Figure 7C; left panel, representative images, and right panel, quantitative results). Treatment with T+E+R+D increased superoxide staining by 178%; however, pretreatment with T-CoQ_{10}-NPs significantly attenuated this effect.

DISCUSSION

The common feature of both untreated and treated HIV infection is the development of comorbidities, including accelerated or accentuated aging.[23,24] For example, a recent study indicated, on the basis of the epigenetic clock, that HIV infection led to an average aging advancement of 4.9 years, increasing the expected mortality risk by 19%.[25] This problem is of great significance because ∼70% of adults with HIV in the US are likely to be 50 or older by the year 2020.[26] The life expectancy of a 20-year-old HIV-positive adult on ART is expected to be ∼70 years.[27,28] Among comorbidities experienced by older HIV-infected individuals, different forms of HANDs are detected in ∼30−50% of infected patients[29] and are more advanced in older patients.[11,12,30−32] In fact, advanced age is one of the demographic factors associated with increased risk of neurocognitive decline and susceptibility to HANDs.[31,33,34] Several factors may be responsible for this phenomenon, including persistent (albeit at low level) HIV replication in the CNS,[4] increased deposition of amyloid in HIV-infected brains,[33] low levels of chronic neuroinflammation,[12,34] and the impact of HIV proteins, such as Tat and gp120.[35,36] However, HIV comorbidities, such as accelerated aging, are likely to be driven not only by HIV itself but also by the toxicity associated with long-term use of ART. Indeed, the use of ART has reduced the severity of neurological diseases but has not affected their prevalence.[37]

Antiretroviral drugs have restricted the capability of crossing the BBB and reaching therapeutic concentrations in the CNS. Several efflux pumps, such as P-gp and organic anion transporters, can actively remove these therapeutics out of the CNS. In addition, antiretroviral drugs that are highly bound to plasma proteins are less likely to cross the BBB. Low molecular weight and hydrophobicity of drugs are factors that promote BBB penetration, while ionization has a negative effect. In addition, multiple mechanisms can play roles in the ability of drugs to cross into the brain parenchyma. They include the paracellular aqueous pathway, the transcellular lipophilic pathway, transport proteins, receptor mediated transcytosis, and adsorptive transcytosis.[38] Because of these factors, antiretroviral drugs do not reach effective therapeutic concentrations in the brain, contributing to the development of drug resistance[39] and/or formation of HIV reservoirs in the CNS. To circumvent these limitations, the CNS penetration-effectiveness (CPE) score was developed as a predictor for therapeutic success of antiretroviral drugs in the brain. In the present study, we used drugs of low to medium CPE scores. Their concentrations were typical for therapeutic plasma levels and higher than the reported concentrations in the cerebral spinal fluid.[40−43] All concentrations were considerably lower than CNS reported toxic levels. In addition, it has also been recognized that antiretroviral drugs undergo various modifications in order to exert antiretroviral activity. For instance, both Tenofovir and Emtricitabine undergo phosphorylation, while Ritonavir and Darunavir follow oxidation pathways.[44] Even though all of the metabolite versions of the antiretroviral drugs that are generated in the liver might not be present in a cellular model, NPCs have been shown to have active drug metabolism capabilities[45] and have been recognized as a good predictor model for drug screening.[46]

Studies have emphasized that balancing the risks and gains of ART has to be considered in order to maximize the positive effects of antiretroviral treatment.[13] Nevertheless, these concerns have not been extensively explored in regard to the impact of ART on the biology and function of NPCs. These cells appear to play a critical role in the biology of HIV infection, as they are prone to HIV infection[47] and their dysfunction may contribute to cognitive decline, especially in the context of aging.[48] Hence, it was striking to observe that exposure to nearly all ART combinations evaluated in the present study resulted in increased ROS generation, mitochondrial dysfunction, and accelerated NPC senescence.

Several therapeutically relevant ART combinations were employed in the current study at the concentrations that have been established to be clinically effective in suppressing HIV replication. Specifically, the combination of Tenofovir and Emtricitabine, both of which are nucleoside reverse transcriptase inhibitors (NRTIs), is recommended as the first treatment option in antiretroviral-naive patients. This drug combination is marketed under the name of Truvada, and it is now approved for pre-exposure prophylaxis (PrEP). Truvada is endorsed for healthy people who are at high risk for HIV infection to lower the probability of getting infected. Thus, the impact of ART on aging, independent of HIV infection, is likely to become an emerging problem in subjects who are prescribed ART for PrEP, providing the rationale for the part of our studies that included treatment with ART alone, without prior HIV infection. In addition, the combinations of Tenofovir, Emtricitabine, and Raltegravir (protease inhibitor) or Tenofovir, Emtricitabine, Ritonavir, and Darunavir (integrase inhibitors) are frequent treatment options in antiretroviral drug experienced patients. Because virtually all HIV patients in the US are on ART and have suppressed viral replication, ART, and not active infection, may be the main factor contributing to their accelerated aging. Thus, HIV replication and ART may independently stimulate accelerated aging in infected patients.

HIV-induced dysfunction of mitochondria in various cells and tissues has been reported in the literature.[35,49,50] For example, HIV gp120 and Tat proteins have been shown to influence the oxidative metabolism and/or interfere with cell proliferation, partially via alterations of mitochondrial functions.[51,52] However, to our knowledge, there is no published data that has studied the link between mitochondrial function in HIV-

DOI: 10.1021/acs.molpharmaceut.8b01014
Mol. Pharmaceutics 2019, 16, 724−736

infected and/or ART-exposed NPCs in the context of cellular senescence. The only recently published study on mitochondrial function and loss of proliferation of NPCs was related to the toxicity of Efavirenz, a drug that belongs to the non-nucleoside reverse transcriptase class of antiretrovirals.[53] While Efavirenz was not part of the ART mixtures in our experiments, the reported data that Efavirenz reduced ATP production and perturbed MMP aligns with the results of the present study. We have found that all combinations of antiretrovirals used in the current study exerted various toxic effects to NPCs. While the mix of Tenofovir and Emtricitabine appeared to be the safest of the drug combinations tested, it still increased generation of ROS in NPCs and induced hyperpolarization of the mitochondrial membrane (Figures 1 and 2). Moreover, the combination that included Tenofovir, Emtricitabine, Ritonavir, and Darunavir was the most toxic, affecting mitochondrial functions to the highest degree. The combination of hyperpolarized mitochondria with low ATP output reported in the current study suggests reversed action of ATP synthase or, alternatively, inhibition of complex I activity which further decreases the oxygen consumption by subsequent complexes and results in decreased ATP levels without altered function of ATP synthase.[54]

A striking finding of the present study was reduced NPC proliferation, combined with accelerated senescence in response to ART. The importance of this finding stems from the fact that NPCs are a renewable source of neuronal cells in the brain. They can migrate to sites of oxidative stress and injury and be incorporated into neuronal networks, replacing damaged neurons. However, this process is not fully sustainable throughout the life span, and exhaustion of NPCs is an important and typical component of aging. The life-long persistence of these cells makes them particularly susceptible to the accumulation of cellular damage, which may lead to cell death, senescence, or loss of regenerative function. NPCs undergo profound changes with age, exhibiting blunted responsiveness to tissue injury, dysregulation of proliferative activities, and declining functional capacities, translating into reduced effectiveness of cell replacement.[55] The impact of ART on metabolic perturbations and oxidative stress of NPCs observed in our experiments may influence NPC exhaustion, contributing to accentuated aging and the development of cognitive decline over time. Importantly, the presented results indicate that ART-induced NPC senescence is preceded by compromised mitochondrial function and that adequate protection against mitochondrial dysfunction can attenuate the progression of NPCs to senescence. The general link between mitochondrial dysfunction and senescence has been recognized in the literature, and its mechanistic intricacies are being studied.[56−58] Our observations on the impact of ART on mitochondrial functions are consistent with a recent report in which the combination of antiretrovirals Tenofovir, Emtricitabine, and Raltegravir led to decreased proliferation of NPCs via induction of apoptosis.[59] Furthermore, the increase in senescence-associated beta-galactosidase activity observed in the present study suggests that there may be increased lysosomal activity in the cells. We, and others, have shown that selected antiretroviral drugs, such as Efavirenz, can promote autophagy.[60,61] Moreover, evidence indicates that senescence may dysregulate mitophagy and induce accumulation of mitochondrial mass.[62] In contrast, it has also been reported that mitochondrial biogenesis is reduced in cells that have a low activity of telomerase.[63] Consistent with these observations, we observed an apparent decrease in mitochondrial mass, as visualized by Mitotracker as part of our SIRT3 immunofluorescence staining (Figure 7A).

HIV-infected individuals are likely to remain on ART for life, emphasizing the importance of developing effective strategies to ameliorate side effects associated with the therapy. Consistent with this notion, we introduced a novel approach to protect against ART-induced cell senescence by mitochondrial-targeted delivery of antioxidant CoQ_{10}. In addition to being a ROS scavenger, CoQ_{10} is also a member of the mitochondrial electron transport chain. Hence, we hypothesized that CoQ_{10}, when loaded into nanoparticles (CoQ_{10}-NPs) and supplemented to dysfunctional mitochondria, may provide a bypass that maintains proper mitochondrial function and consequently halts progression to senescence.

The obtained results indicated the highly protective impact of CoQ_{10}-NPs on both ART-induced mitochondrial dysfunction and NPC senescence. Interestingly, both targeted and nontargeted mitochondrial delivery of CoQ_{10}-NPs protected against ART-induced ROS generation, as measured by DCF fluorescence (Figure 1). However, these results may be connected to the limitation of the method of ROS detection used in the present study. Specifically, DCF fluorescence detects a variety of ROS, except superoxide radicals that are effectively produced in the mitochondria via dysfunction of the oxidative transport chain. Thus, targeted CoQ_{10}-NP delivery might have been more efficient in antioxidant protection as compared to nontargeted delivery; however, this protective impact was not apparent when assessing DCF fluorescence. On the other hand, therapeutic impact of targeted vs nontargeted delivery of CoQ_{10} was clearly distinguished when assessing ART-induced NPC senescence, providing important proof-of-concept evidence that there is a link between mitochondrial dysfunction and accelerated NPC senescence. While literature evidence supports antioxidant properties of CoQ_{10}, especially in the context of mitochondrial-associated injury,[64,65] its targeted nanoparticle delivery allowed us to decrease therapeutic levels to as low as 500 nM. Nevertheless, it is important to note that attenuation of the ART-induced effects was achieved only when adding CoQ_{10} as pretreatment.

Searching for the potential targets responsible for ART-induced mitochondrial dysregulation prompted us to evaluate the expression of SIRT3, a member of the sirtuin family of proteins that is specific to mitochondria. SIRT3 is a NAD-dependent deacetylase that was shown to be an essential part of the mitochondrial ROS maintenance and to decelerate senescence and aging-associated degeneration.[66−68] Part of this protective effect is connected to diminishing activation of redox-activated nuclear factor-κB (NF-κB) and NF-κB-driven inflammatory responses which has been shown in cardiomyocytes.[69] Therefore, it was important that exposure to ART markedly decreased expression of SIRT3 in NPCs and that mitochondria-targeted CoQ_{10} delivery protected against this effect.

CONCLUSION

The study demonstrates that exposure to ART can promote NPC senescence by inducing cellular oxidative stress that results in mitochondrial dysfunction. This impact can be successfully attenuated by supplementing the antiretroviral treatment with mitochondria-targeted delivery of CoQ_{10} using nanoparticles.

DOI: 10.1021/acs.molpharmaceut.8b01014
Mol. Pharmaceutics 2019, 16, 724−736

AUTHOR INFORMATION

Corresponding Author

*Address: Department of Biochemistry and Molecular Biology, University of Miami School of Medicine, Gautier Bldg., Room 528, 1011 NW 15th Street, Miami, FL 33136. Phone: 305-243-0230. E-mail: mtoborek@med.miami.edu.

ORCID

Shanta Dhar: 0000-0003-3042-5272

Michal Toborek: 0000-0003-4475-2119

Author Contributions

M.V. designed and conducted experiments, analyzed data, and wrote the manuscript; B.S. synthesized nanoparticles; S.D. designed and supervised nanoparticle synthesis and provided intellectual input for the Seahorse experiments; M.T. and M.N. provided directions for experimental design, intellectual input, supervision, and resources for all experiments. All authors reviewed and edited the final manuscript.

Notes

The authors declare no competing financial interest.

ACKNOWLEDGMENTS

Supported in part by the National Institutes of Health (NIH), grants HL126559, DA039576, MH098891, MH072567, DA040537, and DA044579. M.V. would like to thank Drs. Diana Avila, Luc Bertrand, and Marta Skowronska for technical support and Dr. Richard Myers for encouragement and academic support.

IMPORTANT ABBREVIATIONS

ART, antiretroviral therapy; CoQ_{10}, coenzyme Q_{10}; D, Darunavir; E, Emtricitabine; HANDs, HIV-associated neurocognitive disorders; NPs, nanoparticles; NPCs, neural progenitor cells; NT-CoQ_{10}-NPs, nontargeted nanoparticles loaded with CoQ_{10}; R, Ritonavir; Ral, Raltegravir; ROS, reactive oxygen species; T, Tenofovir; T-CoQ_{10}-NPs, mitochondria-targeted nanoparticles loaded with CoQ_{10}

REFERENCES

(1) Watkins, C.; Treisman, J. Cognitive impairment in patients with AIDS − prevalence and severity. *HIV/AIDS* **2015**, *7*, 35−47.

(2) Sacktor, N.; Nakasujja, N.; Skolasky, R.; Robertson, K.; Wong, M.; Musisi, S.; Ronald, A.; Katabira, E. Antiretroviral therapy improves cognitive impairment in HIV+ individuals in sub-saharan Africa. *Neurology* **2006**, *67*, 311−314.

(3) Guaraldi, G.; Orlando, G.; Zona, S.; Menozzi, M.; Carli, F.; Garlassi, E.; Berti, A.; Rossi, E.; Roverato, A.; Palella, F. Premature age-related comorbidities among HIV-infected persons compared with the general population. *Clin. Infect. Dis.* **2011**, *53*, 1120−1126.

(4) Rothenaigner, I.; Kramer, S.; Ziegler, M.; Wolff, H.; Kleinschmidt, A.; Brack-Werner, R. Long-term HIV-1 infection of neural progenitor populations. *AIDS* **2007**, *21*, 2271−2281.

(5) Jin, J.; Grimmig, B.; Izzo, J.; Brown, L. A.; Hudson, C.; Smith, A. J.; Tan, J.; Bickford, P. C.; Giunta, B. HIV non-nucleoside reverse transcriptase inhibitor efavirenz reduces neural stem Cell Proliferation In Vitro and In Vivo. *Cell Transplant.* **2016**, *25*, 1967−1977.

(6) Rumbaugh, J. A.; Steiner, J.; Sacktor, N.; Nath, A. Developing neuroprotective strategies for treatment of HIV-associated neurocognitive dysfunction. *Future HIV Ther.* **2008**, *2*, 271−280.

(7) Ellis, R.; Langford, D.; Masliah, E. HIV and antiretroviral therapy in the brain: neuronal injury and repair. *Nat. Rev. Neurosci.* **2007**, *8*, 33−44.

(8) Martín-Maestro, P.; Gargini, R.; García, E.; Perry, G.; Avila, J.; García-Escudero, V. Slower Dynamics and Aged Mitochondria in Sporadic Alzheimer's Disease. *Oxid. Med. Cell. Longevity* **2017**, *2017*, 9302761.

(9) Hogarth, K. A.; Costford, S. R.; Yoon, G.; Sondheimer, N.; Maynes, J. T. DNM1L Variant Alters Baseline Mitochondrial Function and Response to Stress in a Patient with Severe Neurological Dysfunction. *Biochem. Genet.* **2018**, *56*, 56−77.

(10) Kansaku, K.; Takeo, S.; Itami, N.; Kin, A.; Shirasuna, K.; Kuwayama, T.; Iwata, H. Maternal aging affects oocyte resilience to carbonyl cyanide-m-chlorophenylhydrazone-induced mitochondrial dysfunction in cows. *PLoS One* **2017**, *12*, No. e0188099.

(11) Chan, P.; Hellmuth, J.; Spudich, S.; Valcour, V. Cognitive Impairment and Persistent CNS Injury in Treated HIV. *Curr. HIV/AIDS Rep.* **2016**, *13*, 209−217.

(12) Gill, A. J.; Kolson, D. L. Chronic inflammation and the role for cofactors (hepatitis C, drug abuse, antiretroviral drug toxicity, aging) in HAND persistence. *Curr. HIV/AIDS Rep.* **2014**, *11*, 325−335.

(13) Robertson, K.; Liner, J.; Meeker, R. B. Antiretroviral neurotoxicity. *J. NeuroVirol.* **2012**, *18*, 388−399.

(14) Duberley, K. E.; Heales, S. J.; Abramov, A. Y.; Chalasani, A.; Land, J. M.; Rahman, S.; Hargreaves, I. P. Effect of Coenzyme Q10 supplementation on mitochondrial electron transport chain activity and mitochondrial oxidative stress in Coenzyme Q10 deficient human neuronal cells. *Int. J. Biochem. Cell Biol.* **2014**, *50*, 60−63.

(15) Tian, G.; Jinko, S.; Hiroshi, K.; Shin-ya, N.; Shigenari, H.; Nobuyoshi, S.; Hidekane, Y.; Mineko, T.; Yaoyong, W.; Yingye, L.; Hongming, L.; Zhe, X.; Masayuki, M.; Mitsuaki, K.; Kazunori, H.; Toshio, T.; Shin-ichi, U.; Keiichi, H. Ubiquinol-10 Supplementation Activates Mitochondria Functions to Decelerate Senescence in Senescence-Accelerated Mice. *Antioxid. Redox Signaling* **2014**, *20*, 2606−2620.

(16) Skowronska, M.; McDonald, M.; Velichkovska, M.; Leda, A. R.; Park, M.; Toborek, M. Methamphetamine increases HIV infectivity in neural progenitor cells. *J. Biol. Chem.* **2018**, *293*, 296−31.

(17) Cho, H. J.; Kuo, A.; Bertrand, L.; Toborek, M. HIV Alters Gap Junction-Mediated Intercellular Communication in Human Brain Pericytes. *Front. Mol. Neurosci.* **2017**, *10*, 410.

(18) Marrache, S.; Dhar, S. Engineering of blended nanoparticle platform for delivery of mitochondria-acting therapeutics. *Proc. Natl. Acad. Sci. U. S. A.* **2012**, *109*, 16288−16293.

(19) Feldhaeusser, B.; Platt, S. R.; Marrache, S.; Kolishetti, N.; Pathak, R. K.; Montgomery, D. J.; Reno, L. R.; Howerth, E.; Dhar, S. Evaluation of nanoparticle delivered cisplatin in beagles. *Nanoscale* **2015**, *7*, 13822−13830.

(20) Marrache, S.; Tundup, S.; Harn, D. A.; Dhar, S. Ex vivo programming of dendritic cells by mitochondria-targeted nanoparticles to produce interferon-gamma for cancer immunotherapy. *ACS Nano* **2013**, *7*, 7392−7402.

(21) Marrache, S.; Pathak, R. K.; Dhar, S. Detouring of cisplatin to access mitochondrial genome for overcoming resistance. *Proc. Natl. Acad. Sci. U. S. A.* **2014**, *111*, 10444−10449.

(22) Surnar, B.; Basu, U.; Banik, B.; Ahmad, A.; Marples, B.; Kolishetti, N.; Dhar, S. Nanotechnology-mediated crossing of two impermeable membranes to modulate the stars of the neurovascular unit for neuroprotection. *Proc. Natl. Acad. Sci. U. S. A.* **2018**, *115*, E12333−E12342.

(23) Pathai, S.; Bajillan, H.; Landay, A. L.; High, K. P. Is HIV a model of accelerated or accentuated aging? *J. Gerontol., Ser. A* **2014**, *69*, 833−842.

(24) Cysique, L. A.; Brew, B. J. The effects of HIV and aging on brain functions: proposing a research framework and update on last 3 years' findings. *Curr. Opin. HIV AIDS* **2014**, *9*, 355−364.

(25) Gross, A. M.; Jaeger, P. A.; Kreisberg, J. F.; Licon, K.; Jepsen, K. L.; Khosroheidari, M.; Morsey, B. M.; Swindells, S.; Shen, H.; Ng, C. T.; Flagg, K.; Chen, D.; Zhang, K.; Fox, H. S.; Ideker, T. Methylome-wide Analysis of Chronic HIV Infection Reveals Five-Year Increase in Biological Age and Epigenetic Targeting of HLA. *Mol. Cell* **2016**, *62*, 157−168.

(26) United States Senate Special Committee on Aging, 2013. Hearing: Older Americans: The Changing Face of HIV/AIDS in

DOI: 10.1021/acs.molpharmaceut.8b01014
Mol. Pharmaceutics 2019, 16, 724−736

America. One Hundred Thirteenth Congress, first session, September 18, 2013. Washington, D.C.
(27) Samji, H.; Cescon, A.; Hogg, R. S.; Modur, S. P.; Althoff, K. N.; Buchacz, K.; Burchell, A. N.; Cohen, M.; Gebo, K. A.; Gill, M. J.; Justice, A.; Kirk, G.; Klein, M. B.; Korthuis, P. T.; Martin, J.; Napravnik, S.; Rourke, S. B.; Sterling, T. R.; Silverberg, M. J.; Deeks, S.; Jacobson, L. P.; Bosch, R. J.; Kitahata, M. M.; Goedert, J. J.; Moore, R.; Gange, S. J. Closing the gap: increases in life expectancy among treated HIV-positive individuals in the United States and Canada. *PLoS One* **2013**, *8*, No. e81355.
(28) Antiretroviral Therapy Cohort Collaboration. Life expectancy of individuals on combination antiretroviral therapy in high-income countries: a collaborative analysis of 14 cohort studies. *Lancet* **2008**, *372*, 293−299.
(29) Heaton, R. K.; Clifford, D. B.; Franklin, D. R., Jr.; Woods, S. P.; Ake, C.; Vaida, F.; Ellis, R. J.; Letendre, S. L.; Marcott, e T. D.; Atkinson, J. H.; Rivera-Mindt, M.; Vigil, O. R.; Taylor, M. J.; Collier, A. C.; Marra, C. M.; Gelman, B. B.; McArthur, J. C.; Morgello, S.; Simpson, D. M.; McCutchan, J. A.; Abramson, I.; Gamst, A.; Fennema-Notestine, C.; Jernigan, T. L.; Wong, J.; Grant, I.; CHARTER Group. HIV-associated neurocognitive disorders persist in the era of potent antiretroviral therapy: CHARTER Study. *Neurology* **2010**, *75*, 2087−2096.
(30) Greene, M.; Covinsky, K. E.; Valcour, V.; Miao, Y.; Madamba, J.; Lampiris, H.; Cenzer, I. S.; Martin, J.; Deeks, S. G. Geriatric syndromes in older HIV-infected adults. *JAIDS, J. Acquired Immune Defic. Syndr.* **2015**, *69*, 161−167.
(31) Jahanshad, N.; Valcour, V. G.; Nir, T. M.; Kohannim, O.; Busovaca, E.; Nicolas, K.; Thompson, P. M. Disrupted brain networks in the aging HIV+ population. *Brain Connect.* **2012**, *2*, 335−344.
(32) Becker, J. T.; Sanders, J.; Madsen, S. K.; Ragin, A.; Kingsley, L.; Maruca, V.; Cohen, B.; Goodkin, K.; Martin, E.; Mille, r E. N.; Sacktor, N.; Alger, J. R.; Barker, P. B.; Saharan, P.; Carmichael, O. T.; Thompson, P. M. Subcortical brain atrophy persists even in HAART-regulated HIV disease. *Brain. Imaging Behav.* **2011**, *5*, 77−85.
(33) Wendelken, L. A.; Valcour, V. Impact of HIV and aging on neuropsychological function. *J. NeuroVirol.* **2012**, *18*, 256−263.
(34) Nasi, M.; De Biasi, S.; Gibellini, L.; Bianchini, E.; Pecorini, S.; Bacca, V.; Guaraldi, G.; Mussini, C.; Pinti, M.; Cossarizza, A. Ageing and inflammation in patients with HIV infection. *Clin. Exp. Immunol.* **2017**, *187*, 44−52.
(35) Avdoshina, V.; Fields, J. A.; Castellano, P.; Dedoni, S.; Palchik, G.; Trejo, M.; Adame, A.; Rockenstein, E.; Eugenin, E.; Masliah, E.; Mocchetti, I. The HIV Protein gp120 Alters Mitochondrial Dynamics in Neurons. *Neurotoxic. Res.* **2016**, *29*, 583−593.
(36) Pu, H.; Tian, J.; Andras, I. E.; Hayashi, K.; Flora, G.; Hennig, B.; Toborek, M. HIV-1 Tat protein-induced alterations of ZO-1 expression are mediated by redox-regulated ERK 1/2 activation. *J. Cereb. Blood Flow Metab.* **2005**, *25*, 1325−1335.
(37) Robertson, K. R.; Smurzynski, M.; Parsons, T. D.; Wu, K.; Bosch, R. J.; Wu, J.; McArthur, J. C.; Collier, A. C.; Evans, S. R.; Ellis, R. J. The prevalence and incidence of neurocognitive impairment in the HAART era. *AIDS* **2007**, *21*, 1915−1921.
(38) Bertrand, L.; Nair, M.; Toborek, M. Solving the Blood-Brain Barrier Challenge for the Effective Treatment of HIV Replication in the Central Nervous System. *Curr. Pharm. Des.* **2016**, *22*, 5477−5486.
(39) Ferretti, F.; Gisslen, M.; Cinque, P.; Price, R. W. Cerebrospinal fluid HIV escape from antiretroviral therapy. *Curr. HIV/AIDS Rep.* **2015**, *12*, 280−288.
(40) Droste, J. A.; Verweij-van Wissen, C. P.; Kearney, B. P.; Buffels, R.; Vanhorssen, P. J.; Hekster, Y. A.; Burger, D. M. Pharmacokinetic study of tenofovir disoproxil fumarate combined with rifampin in healthy volunteers. *Antimicrob. Agents Chemother.* **2005**, *49*, 680−684.
(41) Boffito, M.; Jackson, A.; Amara, A.; Back, D.; Khoo, S.; Higgs, C.; Seymour, N.; Gazzard, B.; Moyle, G. Pharmacokinetics of once-daily darunavir-ritonavir and atazanavir-ritonavir over 72 h following drug cessation. *Antimicrob. Agents Chemother.* **2011**, *55*, 4218−4223.
(42) Cusini, A.; Vernazza, P. L.; Yerly, S.; Decosterd, L. A.; Ledergerber, B.; Fux, C. A.; Rohrbach, J.; Widmer, N.; Hirschel, B.; Gaudenz, R.; Cavassini, M.; Klimkait, T.; Zenger, F.; Gutmann, C.; Opravil, M.; Günthard, H. F. Swiss HIVCohort Study. Higher CNS penetration-effectiveness of long-term combination antiretroviral therapy is associated with better HIV-1 viral suppression in cerebrospinal fluid. *JAIDS, J. Acquired Immune Defic. Syndr.* **2013**, *62*, 28−35.
(43) Martínez-Rebollar, M.; Muñoz, A.; Pérez, I.; Hidalgo, S.; Brunet, M.; Laguno, M.; González, A.; Calvo, M.; Loncà, M.; Blanco, J. L.; Martínez, E.; Gatell, J. M.; Mallolas, J. Pharmacokinetic study of dual therapy with raltegravir 400 mg twice daily and Darunavir/Ritonavir 800/100 mg once daily in HIV-1-infected patients. *Ther. Drug Monit.* **2013**, *35*, 552−556.
(44) Varga, A.; Lionne, C.; Roy, B. Twenty-six years of HIV science: an overview of anti-HIV drugs metabolism. *Curr. Drug Metab.* **2016**, *17*, 237−252.
(45) Bond, A. M.; Ming, G. L.; Song, H. Adult mammalian neural stem cells and neurogenesis: five decades later. *Cell Stem Cell* **2015**, *17*, 385−395.
(46) Lorenz, C.; Lesimple, P.; Bukowiecki, R.; Zink, A.; Inak, G.; Mlody, B.; Singh, M.; Semtner, M.; Mah, N.; Auré, K.; Leong, M.; Zabiegalov, O.; Lyras, E. M.; Pfiffer, V.; Fauler, B.; Eichhorst, J.; Wiesner, B.; Huebner, N.; Priller, J.; Mielke, T.; Meierhofer, D.; Izsvák, Z.; Meier, J. C.; Bouillaud, F.; Adjaye, J.; Schuelke, M.; Wanker, E. E.; Lombès, A.; Prigione, A. Human iPSC-derived neural progenitors are an effective drug discovery model for neurological mtDNA disorders. *Cell Stem Cell* **2017**, *20*, 659−674.
(47) Schwartz, L.; Civitello, L.; Dunn-Pirio, A.; Ryschkewitsch, S.; Berry, E.; Cavert, W.; Kinzel, N.; Lawrence, D. M.; Hazra, R.; Major, E. O. Evidence of human immunodeficiency virus type 1 infection of nestin-positive neural progenitors in archival pediatric brain tissue. *J. NeuroVirol.* **2007**, *13*, 274−283.
(48) Artegiani, B.; Calegari, F. Age-related cognitive decline: Can neural stem cells help us? *Aging* **2012**, *4*, 176−186.
(49) Garrabou, G.; Lopez, S.; Moren, C.; Martinez, E.; Fontdevila, J.; Cardellach, F.; Gatell, J. M.; Miro, O. Mitochondrial damage in adipose tissue of untreated HIV-infected patients. *AIDS* **2011**, *25*, 165−170.
(50) Norman, J. P.; Perry, S. W.; Reynolds, H. M.; Kiebala, M.; De Mesy Bentley, K. L.; Trejo, M.; Volsky, D. J.; Maggirwar, S. B.; Dewhurst, S.; Masliah, E.; Gelbard, H. A. HIV-1 Tat Activates Neuronal Ryanodine Receptors with Rapid Induction of the Unfolded Protein Response and Mitochondrial Hyperpolarization. *PLoS One* **2008**, *3*, No. e3731.
(51) Stevens, P. R.; Gawryluk, J. W.; Hui, L.; Chen, X.; Geiger, J. D. Creatine protects against mitochondrial dysfunction associated with HIV-1 Tat-induced neuronal injury. *Curr. HIV Res.* **2015**, *12*, 378−387.
(52) Ma, R.; Yang, L.; Niu, F.; Buch, S. HIV Tat-Mediated Induction of Human Brain Microvascular Endothelial Cell Apoptosis Involves Endoplasmic Reticulum Stress and Mitochondrial Dysfunction. *Mol. Neurobiol.* **2016**, *53*, 132−142.
(53) Jin, J.; Grimmig, B.; Izzo, J.; Brown, L. A. M.; Hudson, C.; Smith, A. J.; Tan, J.; Bickford, P. C.; Giunta, B. HIV Non-Nucleoside Reverse Transcriptase Inhibitor Efavirenz Reduces Neural Stem Cell Proliferation In Vitro and In Vivo. *Cell Transplant.* **2016**, *25*, 1967−1977.
(54) Forkink, M.; Manjeri, G. R.; Liemburg-Apers, D. C.; Nibbeling, E.; Blanchard, M.; Wojtala, A.; Smeitink, J. A. M.; Wieckowski, M. R.; Willems, P. H. G. M.; Koopman, W. J. H. Mitochondrial hyperpolarization during chronic complex I inhibition is sustained by low activity of complex II, III, IV and V. *Biochim. Biophys. Acta, Bioenerg.* **2014**, *1837*, 1247−1256.
(55) Oh, J.; Lee, Y. D.; Wagers, A. J. Stem cell aging: mechanisms, regulators and therapeutic opportunities. *Nat. Med.* **2014**, *20*, 870−880.
(56) Giorgi, C.; Marchi, S.; Simoes, I. C. M.; Ren, Z.; Morciano, G.; Perrone, M.; Patalas-Krawczyk, P.; Borchard, S.; Jedrak, P.; Pierzynowska, K.; Szymanski, J.; Wang, D. Q.; Portincasa, P.; Wegrzyn, G.; Zischka, H.; Dobrzyn, P.; Bonora, M.; Duszynski, J.; Rimessi, A.; Karkucinska-Wieckowska, A.; Dobrzyn, A.; Szabadkai, G.; Zavan, B.; Oliveira, P. J.; Sardao, V. A.; Pinton, P.; Wieckowski, M. R. Mitochondria and Reactive Oxygen Species in Aging and Age-Related Diseases. *Int. Rev. Cell Mol. Biol.* **2018**, *340*, 209−344.

DOI: 10.1021/acs.molpharmaceut.8b01014
Mol. Pharmaceutics 2019, 16, 724−736

(57) Wiley, C. D.; Velarde, M. C.; Lecot, P.; Liu, S.; Sarnoski, E. A.; Freund, A.; Shirakawa, K.; Lim, H. W.; Davis, S. S.; Ramanathan, A.; Gerencser, A. A.; Verdin, E.; Campisi, J. Mitochondrial Dysfunction Induces Senescence with a Distinct Secretory Phenotype. *Cell Metab.* **2016**, *23*, 303−314.
(58) Wiley, C. D.; Campisi, J. From Ancient Pathways to Aging Cells-Connecting Metabolism and Cellular Senescence. *Cell Metab.* **2016**, *23*, 1013−1021.
(59) Xu, P.; Wang, Y.; Qin, Z.; Qiu, L.; Zhang, M.; Huang, Y.; Zheng, J. C. Combined Medication of Antiretroviral Drugs Tenofovir Disoproxil Fumarate, Emtricitabine, and Raltegravir Reduces Neural Progenitor Cell Proliferation In Vivo and In Vitro. *J. Neuroimmune Pharmacol.* **2017**, *12*, 682−692.
(60) Bertrand, L.; Toborek, M. Dysregulation of Endoplasmic Reticulum Stress and Autophagic Responses by the Antiretroviral Drug Efavirenz. *Mol. Pharmacol.* **2015**, *88*, 304−315.
(61) Purnell, P. R.; Fox, H. S. Efavirenz induces neuronal autophagy and mitochondrial alterations. *J. Pharmacol. Exp. Ther.* **2014**, *351*, 250−258.
(62) Korolchuk, V. I.; Miwa, S.; Carroll, B.; von Zglinicki, T. Mitochondria in Cell Senescence: Is Mitophagy the Weakest Link? *EBioMedicine* **2017**, *21*, 7−13.
(63) Sahin, E.; Colla, S.; Liesa, M.; Moslehi, J.; Müller, F. L.; Guo, M.; Cooper, M.; Kotton, D.; Fabian, A. J.; Walkey, C.; Maser, R. S.; Tonon, G.; Foerster, F.; Xiong, R.; Wang, Y. A.; Shukla, S. A.; Jaskelioff, M.; Martin, E. S.; Heffernan, T. P.; Protopopov, A.; Ivanova, E.; Mahoney, J. E.; Kost-Alimova, M.; Perry, S. R.; Bronson, R.; Liao, R.; Mulligan, R.; Shirihai, O. S.; Chin, L.; DePinho, R. A. Telomere dysfunction induces metabolic and mitochondrial compromise. *Nature* **2011**, *470*, 359−65.
(64) Moreira, P. I.; Santos, M. S.; Sena, C.; Nunes, E.; Seiça, R.; Oliveira, C. R. CoQ10 therapy attenuates amyloid beta-peptide toxicity in brain mitochondria isolated from aged diabetic rats. *Exp. Neurol.* **2005**, *196*, 112−119.
(65) Noh, Y. H.; Kim, K. Y.; Shim, M. S.; Choi, S. H.; Choi, S.; Ellisman, M. H.; Weinreb, R. N.; Perkins, G. A.; Ju, W. K. Inhibition of oxidative stress by coenzyme Q10 increases mitochondrial mass and improves bioenergetic function in optic nerve head astrocytes. *Cell Death Dis.* **2013**, *4*, e820.
(66) Ansari, A.; Rahman, M. S.; Saha, S. K.; Saikot, F. K.; Deep, A.; Kim, K. H. Function of the SIRT3 mitochondrial deacetylase in cellular physiology, cancer, and neurodegenerative disease. *Aging Cell* **2017**, *16*, 4−16.
(67) Brown, K.; Xie, S.; Qiu, X.; Mohrin, M.; Shin, J.; Liu, Y.; Zhang, D.; Scadden, D. T.; Chen, D. SIRT3 Reverses Aging-associated Degeneration. *Cell Rep.* **2013**, *3*, 319−327.
(68) Jung, Y. H.; Lee, H. J.; Kim, J. S.; Lee, S. J.; Han, H. J. EphB2 signaling-mediated Sirt3 expression reduces MSC senescence by maintaining mitochondrial ROS homeostasis. *Free Radical Biol. Med.* **2017**, *110*, 368−380.
(69) Chen, C. J.; Fu, Y. C.; Yu, W.; Wang, W. SIRT3 protects cardiomyocytes from oxidative stress-mediated cell death by activating NF-kappaB. *Biochem. Biophys. Res. Commun.* **2013**, *430*, 798−803.

DOI: 10.1021/acs.molpharmaceut.8b01014
Mol. Pharmaceutics 2019, 16, 724−736